



**IAF-97-J.4.01**

**Activities in preparation of the sounding rocket  
experiment on oscillatory Marangoni flow**

**R. Monti, R. Savino, M. Lappa**

Università degli studi di Napoli "Federico II"

Dipartimento di Scienza e Ingegneria dello Spazio "L. G. Napolitano"

**R. Fortezza**

MARS - Microgravity Advanced Research and Support Center

**48th International Astronautical Congress  
October 6-10, 1997/Turin, Italy**

# ACTIVITIES IN PREPARATION OF THE SOUNDING ROCKET EXPERIMENT ON OSCILLATORY MARANGONI FLOW

R.Monti,R.Savino,M.Lappa

Università degli studi di Napoli "Federico II"  
Dipartimento di Scienza e Ingegneria dello Spazio Luigi G.Napolitano

R.Fortezza

Mars Center, Napoli, Italy

## Abstract

The experiment "Pulsating and Rotating instabilities (PULSAR)", to be performed on board the Maxus 3 sounding rocket in spring 1998, is aimed at identifying the features of the oscillatory flow regime that is established in a cylindrical liquid bridge when a sufficiently large temperature difference is imposed between the supporting disks. The investigators intend to confirm previous numerical results that predict for a large Prandtl number liquid a first transition from the axi-symmetric steady to a three-dimensional oscillatory flow, characterized by temperature spots pulsating at fixed positions in the liquid column and then a second transition from the pulsating regime to another model, with temperature spots rotating in the azimuthal direction.

This paper reports on the activity in preparation of the experiment, consisting in extensive numerical simulations, complemented by laboratory experiments performed with a microscale apparatus. The results of the computations and of the microscale experiments define an experimental procedure that makes optimum use of the microgravity time available during the sounding rocket experiment.

## 1.Introduction

The existence of a critical Marangoni number for the onset of the time-dependent asymmetric flow in high Prandtl number fluids has been established two decades ago<sup>7</sup>. In reviewing the past works on the subject one realizes, however, that they mainly consist in evaluating the critical value of the temperature difference across the bridge (that correspond to the transition conditions) and that no effort was made to understand the nature of the transition of Marangoni flow.

In spite of the work done in the past we have only very limited insight of the nature of oscillatory thermocapillary convection. There are no systematic experimental investigation on the spatio-temporal structure of Marangoni flows for imposed temperature differences  $\Delta T \geq \Delta T_c$ .

More recently, oscillatory thermocapillary flows in liquid bridges have been investigated, by the hydrodynamic stability theory<sup>4-5</sup>.

For high Prandtl numbers this theory predicts that the three dimensional supercritical state after the Hopf bifurcation point can be interpreted as a superposition of two counter-propagating waves, characterized by an axial and an azimuthally component, so that the

resulting disturbance exhibits an azimuthal component running under a certain angle against the axis of the bridge.

The superposition of two waves with equal amplitude should result in a "standing wave", with the minimum and maximum disturbances at fixed azimuthal positions; while the superposition of waves with different amplitude should give rise to a "travelling wave", with the minimum and maximum disturbances travelling in azimuthal direction. Unfortunately, nothing can be predicted by the linear stability analyses about the amplitude of these disturbances.

The travelling wave model was observed by different investigators during experimental microgravity research<sup>6-7</sup>. The standing wave model, instead, has been observed more recently only during experimental ground-based activities<sup>8</sup>. However, the relationship between the two flow instabilities mechanisms was never investigated.

More recently the results obtained using a full Navier-Stokes, three-dimensional and time-dependent (Monti-Savino<sup>1</sup>) code able to predict the behaviour of the flow also far from the bifurcation point (the linear stability analyses instead can give information only in a restricted neighbour of the transition point) have shown that the standing wave and travelling wave models are relative to two consecutive bifurcations of the Marangoni flow. The code predicts that for a large Prandtl number liquid the flow is subject to a first transition from the axy-symmetric steady to the three-dimensional oscillatory state, characterized by the appearance of the standing wave instability model and then, after a certain time, to a second transition from the standing wave to the travelling wave model.

To confirm these numerical results an experiment has been proposed by the

authors and selected by the European Space Agency for a Maxus sounding rocket mission. Aim of the experiment is the study of the different flow and temperature distributions of the oscillatory Marangoni convection that can be reached after the onset (i.e. after the bifurcation point).

## **2. Description of the PULSAR sounding rocket experiment**

A silicone oil (5 [cs]) liquid bridge will be suspended between two cylindrical disks of the same diameter. The temperature difference between supports will be varied heating the upper disk and cooling the lower one, with respect to the ambient temperature, with symmetrical temperature ramps. When instability conditions are reached the temperature difference will be held constant in order to sustain the oscillatory flow.

The flow organization will be detected from video images (by following tracers illuminated by a laser sheet in a meridian plane).

The time temperature profiles at four fixed points with the same axial and radial coordinates, at an azimuthal position of 90 degree, will be measured by fine temperature sensors (T1 at  $\varphi=0$ , T2 at  $\varphi=\pi/2$ , T3 at  $\varphi=\pi$ , T4 at  $\varphi=3\pi/2$ ). The surface temperature distribution will be measured by an infrared thermocamera.

The four thermocouples will measure the phase shift between the temperatures at different azimuthally located points. From the analysis of the data shift it is possible to understand if the oscillatory model is pulsatory or rotatory. Moreover the infrared thermocamera will give a direct visualization of the temperature spots on the surface of the bridge that correspond to the minimum and maximum temperature disturbances.

## 2.1 Description of the flight hardware

The experimental model used is an improved version of that already used during previous experiments on Texas and Maxus missions.

A pressurized test cell contains the liquid bridge, formed injecting the silicon oil between two disks 70s after lift-off, when the microgravity conditions are established. The liquid reservoir closed during the acceleration phase, is opened by an electromechanic device and the exact quantity of liquid needed to form a cylindrical liquid bridge is pushed between the two copper disks.

The active cooling and heating system is designed in order to reduce the heat transfer from the oil to the ambient. The system, based on two Peltier elements, allows to control the temperature ramps of the two disks imposing symmetric temperature profiles with respect to the initial temperature; the supports are equipped with thermocouples in order to control the realized  $\Delta T$ .

Two motorized thermocouple combs with four thin sensors placed at four fixed points having the same radial coordinates, but with an azimuthal shift of 90 degree, are used for the analysis of the temperature inside the liquid bridges during the experimental phases (the thermocouples are inserted in the bridge in axial direction through apposite holes in the disks sustaining the bridge).

The liquid motion is visualized using tracers illuminated by two different laser light cuts. The first laser beam is oriented orthogonally to the main optical path of the first CCD. The laser used is He-Ne with a wavelength of 635 nm. The images detect the the tracers motion contained in the cylinder meridian plane of the liquid bridge. An additional laser beam, generated using a diode laser of 675 nm, with an illuminated plane parallel to the

cylindrical liquid bridge generatrix is directed in the central part of the liquid.

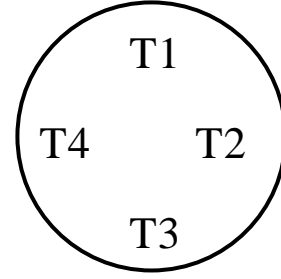


Fig 1: scheme of the thermocouples

## 2.2 The analysis of the oscillatory model

Only two thermocouples are not enough to detect if the oscillatory model is pulsating or rotating.

The linear stability analysis have shown that for large  $Pr$ , the basic Marangoni flow loses its stability to a pair of counterpropagating azimuthal waves. The phase of these waves does not only depend on  $\phi$  and  $t$  but also on the radial and axial coordinates  $r$  and  $z$ . Therefore, the surfaces of constant phase are not vertical planes through the origin. Rather the constant-phase surfaces can be imagined as vertical planes that have been twisted around the vertical axis, the twist being given by a phase  $G(r,z)$ . It turns out that the wave front  $F$  of such hydrothermal waves are inclined with respect to  $z$ :

$$F_{\pm} = A(r, z) \exp\{i[\pm m\mathbf{j} - \omega t + G(r, z)]\}$$

A superposition with an arbitrary amplitude ratio  $\varepsilon \in [0,1]$  (linear stability theory can not evaluate  $\varepsilon$ ) can be written according to Kuhlmann and Rath<sup>9</sup> as

$$F = A(r, z) \left[ (1 + \varepsilon)^2 \cos^2(m\phi - \phi_0) + (1 - \varepsilon)^2 \sin^2(m\phi - \phi_0) \right]^{1/2} e^{i(\phi - \omega t)}$$

$$f = \arctan \left[ \frac{1 - \varepsilon}{1 + \varepsilon} \tan(m\mathbf{j} - \mathbf{j}_0) \right] + G(r, z)$$

In the case of an azimuthally standing wave (same amplitude of the counterpropagating waves and  $\varepsilon=1$ ) the resulting field should be represented by

$$F = A(r, z)2 \cos(m\phi - \phi_0) \cos(\omega t)$$

where the oscillatory term does not depend on  $\phi$ . When oscillatory term does not depend on  $\phi$ , maximum and minimum disturbance are fixed in space and the minimum is continually replaced by the maximum and viceversa as soon as  $\cos(\omega t)$  changes its sign. These extrema in the disturbance distribution give rise to hotter and colder zone in the bridge. In particular for the standing wave model ( $m=1$ ) the three-dimensional temperature disturbance consists of a pair of spots (hot and cold) pulsating at the same azimuthal positions along the interface. At the same time strong interior temperature extrema appear.

When the amplitude of the two hydrothermal waves is not the same ( $\varepsilon \neq 1$ ) the oscillatory term  $\cos(\phi - \omega t)$  depends on  $\phi$  so that the minimum and maximum disturbances travel in azimuthal direction and the phase depends continuously on  $\phi$ .

For  $m = 1$ , in the case of an azimuthally standing wave the phase experiences a jump  $\Delta\phi = \pi$  between two location  $\phi_1 = \phi_0 + \pi/2$ , and  $\phi_2 = \phi_0 - \pi/2$ , but also in the case of a travelling wave two thermocouples having an azimuthal shift of 180 should measure a phase shift of  $\pi$ . The difference between a standing and a travelling wave consists in the fact that in the first case, for  $m=1$ , only two values of the phase shift are allowed ( $\Delta\phi = 0$  if the considered points are placed on the same spot,  $\Delta\phi = \pi$  if the two points belong to two different spots), while in the second case the possible values of the phases are not discrete.

These considerations show hence that only two thermocouples are not enough to understand if the flow field is pulsating or rotatory.

### 3. Activities in preparation of the sounding rocket experiment

While the linear stability theory cannot predict if the instability sets as a standing wave or as a travelling wave, the numerical results of Monti and Savino<sup>1</sup> show that the rotating model is reached only after the pulsating one. Probably this behaviour is due to the fact that in a first phase a superposition of two counter-propagating waves takes place with equal amplitude while in a second phase one of the two waves reaches an amplitude greater than the other one.

However the time necessary to go from the first bifurcation to the second one is not a priori known and depends on several parameters: the fluid, the  $\Delta T$  and the ramping rate of the temperature on the disks.

Numerical experimentation has been completed by laboratory experiments performed with a microscale apparatus.

#### 3.1 Description of the experimental microscale apparatus

A general scheme of the experimental apparatus is illustrated in Fig. 2 .

The experimental facility includes a mechanical support system, a temperature control system, a visualisation system.

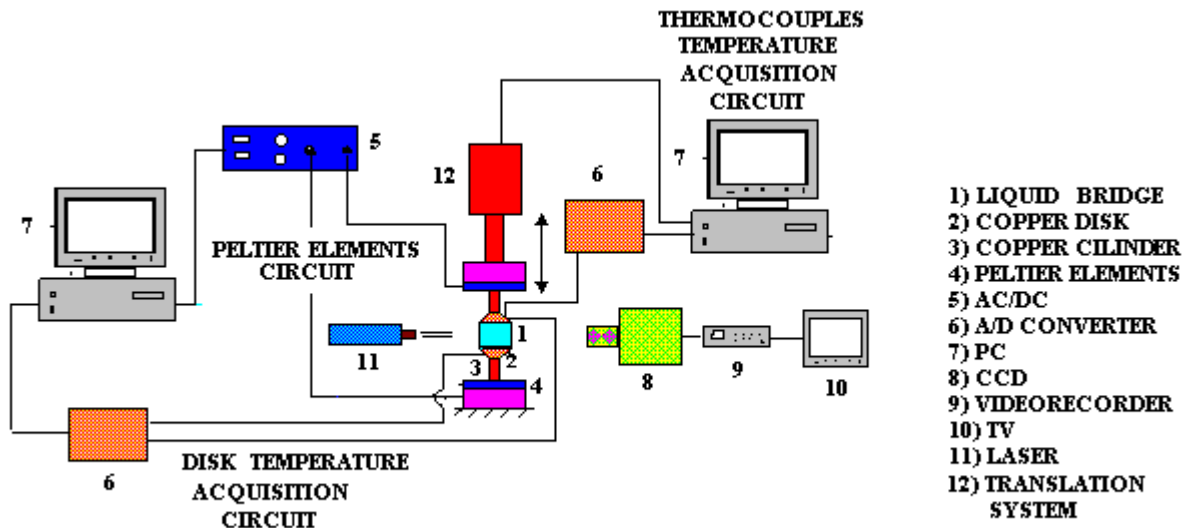


Fig 2: scheme of the microscale experimental apparatus

The support system consists of two cylindrical copper rods that sustain the bridge.

The two rods have the same diameter (4 mm).

The upper disk can be translated along the vertical axis in order to realize a bridge having the desired aspect ratio. The translation is obtained using a motorized micrometer system controlled by a computer.

The temperature control system, that is connected with a tension generator, includes two Peltier elements that establish appropriate temperature on the disks in order to impose the desired temperature differences. Two temperature sensors are located on the disks and connected with a personal computer by means an A/D converter.

One of the two disks sustaining the bridge has four holes having an azimuthal shift of 90 degree and the temperatures near the hot disk have been measured with fine thermocouples inserted into the microzone

through these holes (same technique proposed for the flight experiment).

The signals of these thermocouples have been monitored using a second acquisition circuit (Pc and A/D converter).

The liquid motion in the liquid bridge has been visualized by hollow glass micro spheres (2 to 20  $\mu\text{m}$  in diameter) illuminated by a laser light cut in the meridian plane. A JVC/CCD camera, fixed to the test cell, and a professional video recorder are used to film and record the video images.

### 3.2 On ground experimental results

In these ground experiments the length of the liquid bridge has been kept small mainly to avoid large curvature of the liquid gas interface and to minimize buoyancy effects in the liquid zone. In fact, the ratio of Rayleigh to Marangoni number (that measures the driving actions of the gravity and of the surface tension unbalance) grows in fact quadratically with the linear dimension of the liquid

zone making thermal convection more important for larger liquid volumes. Ground based studies have been carried out hence emphasizing the thermocapillary effect in comparison with the buoyancy effect by reducing the typical scale.

To reproduce on ground conditions similar to the conditions that will set during the flight experiment, some thermodynamic property of the liquid have been changed in the microscale experiments. Since the Marangoni number is one of the parameters governing the nature of the bifurcation, assuming that the derivative of the surface tension  $\sigma_t$ , the density  $\rho$  and the thermal diffusivity  $\alpha$  are constant and considering that the length of the microzone is small compared to the extension of the bridge that will be realized during the  $\mu\text{g}$  experiment, to keep  $\text{Ma}$  ( $\text{Ma} = \frac{\rho\sigma_t\Delta TL}{\alpha\nu}$ )

comparable between the two experiments, the viscosity of the liquid has been scaled down. In particular a 3 [cs] silicone oil microzone has been considered (instead of 5 [cs]).

Also the aspect ratio has been fixed in order to have conditions close to the conditions that will be established during the sounding rocket experiment.

In the experiment to be performed on the sounding rocket  $A = 1$  but in the microscale experiments the aspect ratio has been selected less than unity (in flight conditions  $g$  is 0 the liquid bridge has a cylindrical surface) and greater than 0.5 in order to establish a critical wave number  $m = 1$  (for  $A < 0.5$  the critical wave number is  $m=2$  or higher).

The experimental results indicate that for the microzone considered ( $A=0.75$ ) the critical  $\Delta T$  is 18 K (the zone heated from above in order to minimize the effects of the buoyancy convection).

The signals measured by the four thermocouples show that instability starts as a standing wave model.

In Fig 3 it is evident in fact that there is no phase shift between the temperature signals measured by two thermocouples at 90 degree. The phase shift is instead  $\pi$  when the two considered thermocouples have an azimuthal shift of 180 degree.

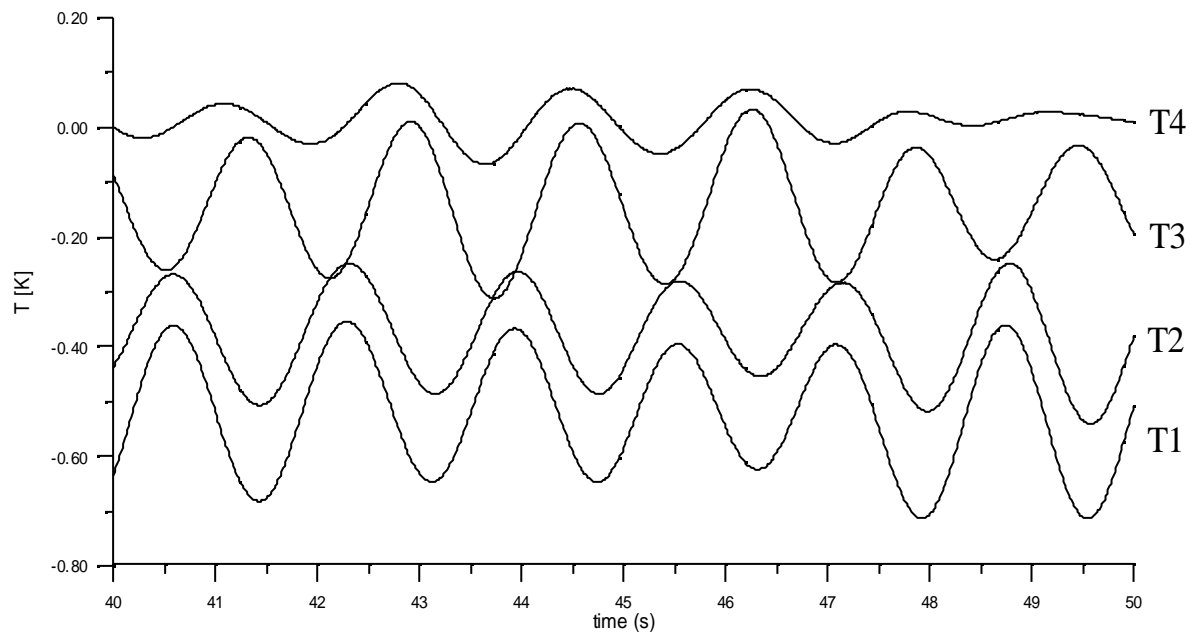


Fig 3: Thermocouple signals ( $\Delta T < 30\text{K}$ )

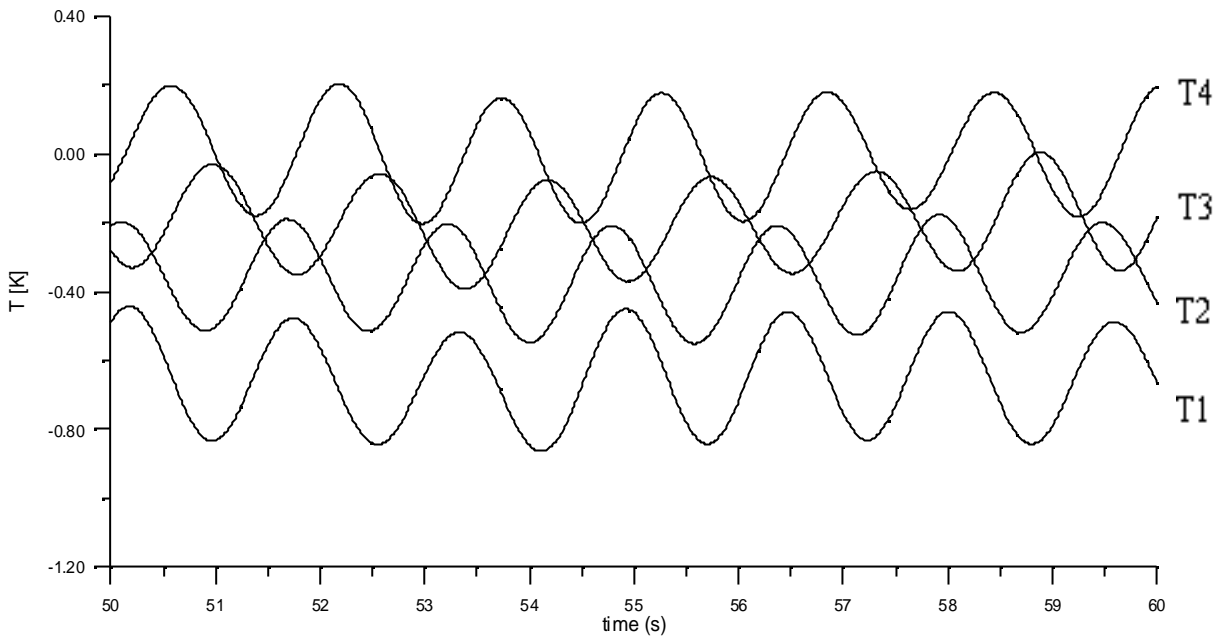


Fig 4: Thermocouple signals ( $\Delta T=30\text{K}$ )

The standing wave model turns into the travelling one a while after the onset (several minutes for the microscale configuration). The experimental results in the case of the microscale show that the transition can be shortened by increasing the  $\Delta T$ .

For  $\Delta T=30\text{K}$  the regime is a travelling wave. In fact two thermocouples having an azimuthal shift of 90 degree (Fig 4) measure signals having a phase shift of  $\pi/2$  and two thermocouples having an azimuthal displacement of 180 degree measure signals having a phase shift of  $\pi$  (i.e the phase depends continuously on the azimuthal coordinate  $\varphi$ ).

The experimental results indicates moreover that an increase of  $\Delta T$  from 20 K to 30 K gives rise to the transition from pulsating to rotating wave but does not affect the wave number.

These results give experimental evidence for the proposed theory (Ref<sup>1</sup>) that the instability of Marangoni flow starts as a standing wave model and than turns in a travelling wave model after a certain time and/or if the critical parameter  $Ma$  is increased.

To investigate the influence of buoyancy forces on the stability and on the bifurcation process we heated the bridge from above and from below. The direct comparison of both heating conditions gives insight into the influence of buoyant forces on unsteady Marangoni convection.

The results indicate that the critical  $\Delta T$  obtained when heating from below are always larger than those found when heating from above. This behaviour is intriguing because when the thermocapillary effect is not present, heating from above yields a stable temperature distribution in the liquid bridge, while heating from below gives rise to an unstable situation and to the onset of convection (in contrast with the generalized idea that heating from below has always a destabilizing effect).

These results are in agreement with those obtained by Velten, Schwabe and Scharmann<sup>7</sup> who observed shifts of the critical Marangoni number for liquid bridges heated from below.

### 3.3 Numerical simulations

To improve on the accuracy of the simulation (in the microscale the effects of gravity are present and therefore some characteristic parameters are different) a 3D numerical computation of the two geometries (microscale and flight floating zone) has been performed by using fluid-dynamic codes.

The problem under investigation consists of a standard half-zone model with rigid surface and time-dependent temperature profiles on the disks ( $T=T_0 \pm R t$ ). The final temperature difference at the end of the ramp will be denoted by  $\Delta T = T_{hot} - T_{cold} = 2 R t_{ramp}$ , where  $R$  is the rate of the ramping and  $t_{ramp}$  is the duration of the ramp. The bridge is characterized by length  $L$ , diameter  $D$  and aspect ratio  $A=L/D$  (Fig 1).

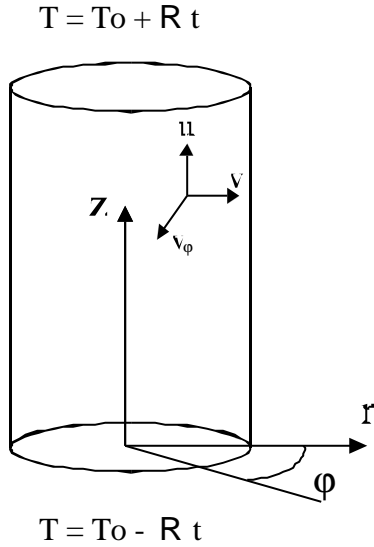


Fig 5: Scheme of the liquid bridge

The flow in the volume phase is governed by the continuity, Navier-Stokes and energy equations :

$$\tilde{N} \times \mathbf{V} = 0 \quad (1a)$$

$$\frac{\rho \mathbf{V}}{t} = -\frac{1}{r} \nabla p - \nabla \cdot \left[ \mathbf{V} \mathbf{V} \right] + \mathbf{u} \nabla^2 \mathbf{V} \quad (1b)$$

$$\frac{\partial T}{\partial t} = -\tilde{N} \times \left[ \mathbf{V} T \right] + \alpha \tilde{N}^2 T \quad (1c)$$

where  $\nu$  and  $\alpha$  are the kinematic viscosity and the thermal diffusivity.

The initial and boundary conditions read:

$$t=0: \mathbf{V}(z, r, \varphi) = T(z, r, \varphi) = 0 \quad (2)$$

$$\underline{\text{cold disk}} \quad 0 \leq r \leq R; 0 \leq \varphi \leq 2\pi$$

$$\mathbf{V}(z=0, r, \varphi, t) = 0; T(z=0, r, \varphi, t) = -R t$$

(3a,b)

$$\underline{\text{hot disk}} \quad 0 \leq r \leq R; 0 \leq \varphi \leq 2\pi$$

$$\mathbf{V}(z=L, r, \varphi, t) = 0; T(z=L, r, \varphi, t) = R t$$

(4a,b)

$$\underline{\text{cylindrical free surface}}: 0 \leq z \leq L; 0 \leq \varphi \leq 2\pi$$

$$v(z, r=R, \varphi, t) = 0 \quad (5)$$

$$\mu \frac{\partial u}{\partial r}(z, r=R, \varphi, t) = -\sigma_T \frac{\partial T}{\partial z}(z, r=R, \varphi, t) \quad (6)$$

$$r \frac{\partial V_\varphi}{\partial r}(z, r=R, \varphi, t) - V_\varphi(z, r=R, \varphi, t) = -\frac{1}{\mu} \sigma_T \frac{\partial T}{\partial \varphi}(z, r=R, \varphi, t) \quad (7)$$

$$\frac{\partial T}{\partial r}(z, r=R, \varphi, t) = 0 \quad (8)$$

The solution method has been described in Ref<sup>1</sup> where an independent validation of the computational model has been carried out comparing the numerical results with other three-dimensional numerical solutions available in literature and with experimental data obtained in microgravity experiments.

$g/g_0$	numerical $\Delta T_c$ [K]	numerical $f$ [Hz]	experimental $\Delta T_c$ [K]	experimental $f$ [Hz]
0	19	0.9	-	-
1	18	1.0	18	0.75
-1	46	2.0	44	1.9

### 3.4 Comparison of the on ground experimental measurements with the numerical predictions

To confirm the result that heating from below has a stabilizing effect on Marangoni convection, the experimental results obtained using the microscale apparatus have been compared with numerical simulations.

There is good agreement between the numerical and experimental values of critical  $\Delta T_c$  and the corresponding frequency.

When heating from above the experimental critical  $\Delta T_c$  is 18 K equal to the numerical one (there is a small difference in the frequencies).

When heating from below the experimental critical  $\Delta T$  becomes 44 K and this behaviour is confirmed by the numerical computation that predicts a critical  $\Delta T = 46$  K.

The numerical computation shows moreover that there is only 1 K difference between the critical  $\Delta T_c$  computed in the case of  $g = 0$  and in the case of  $g = 1$  and bridge heated from above (this shows that when the zone is heated from above, the effects of the buoyancy convection are minimized).

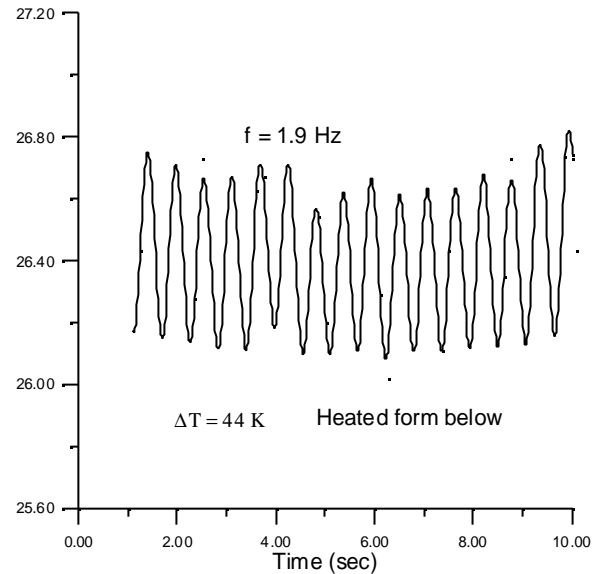


Fig 6

### 3.5 Definition of the flight experimental procedure

The numerical computations show that for the configuration to be investigated during the microgravity experiment, if the imposed temperature difference is sufficiently small (but larger than the critical one), the three-dimensional instability starts (at  $t = 280$  s) as a standing wave ( $m=1$ , where  $m$  is the number of wavelengths of the disturbance on the circumference of the zone that depends on several parameters and in particular on the aspect ratio of the bridge and on the Marangoni number) and the pulsating mechanism last for a time larger than the available microgravity time (about 12 minutes - Fig 7).

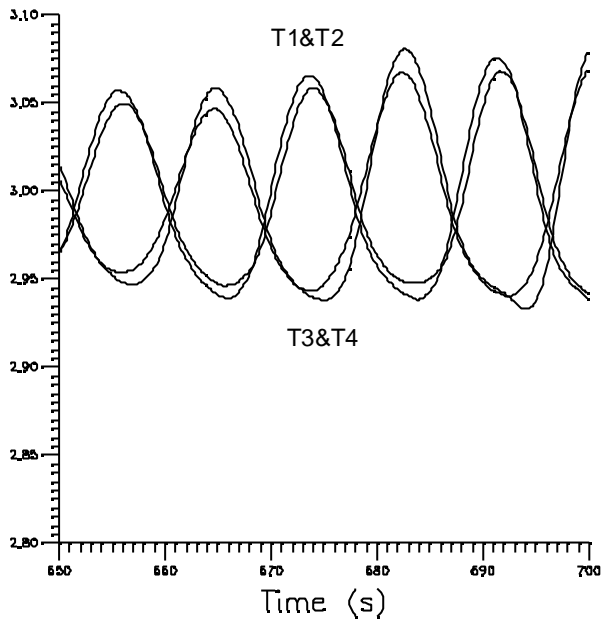


Fig 7: Oscillations at the end of the available microgravity time ( $\Delta T=20$  K)

Conversely, if the imposed temperature difference is sufficiently large (e.g.  $\Delta T > 40$  K) the instability starts (at  $t = 220$  s) as a travelling wave ( $m=1$ ) and no transition can be observed from the pulsating to the rotating instability mechanism (Fig 8).

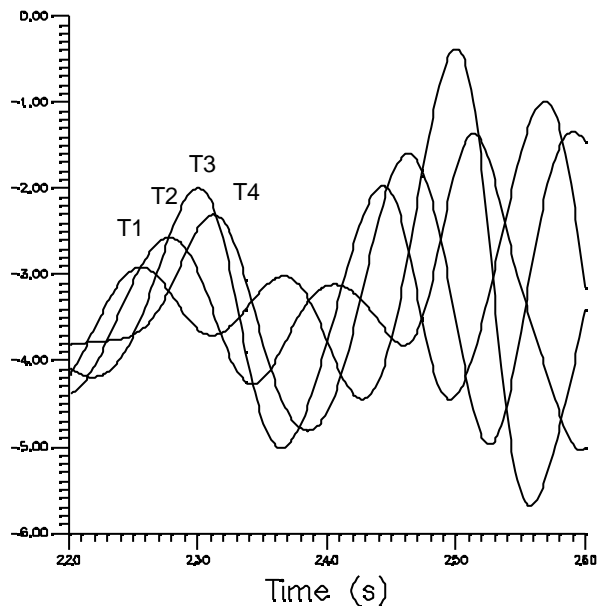


Fig 8: Oscillations at the onset ( $\Delta T=40$  K)

Since the the objective of the experiment is to observe both the pulsating and the rotating instabilities, a different experimental procedure has been investigated numerically: a pulsating instability is first achieved by imposing a suitable temperature difference with a relatively fast temperature ramp (e.g.  $\Delta T=30$  K in 30 [s]); when this oscillatory mechanism is completely developed (Fig 9b) the temperature difference is further increased ( $\Delta T = 40$  K) so that the transition to the rotating instability is accelerated.

For  $\Delta T = 30$  K, the instability sets as a standing wave model ( $m=1$ ) and the three-dimensional temperature disturbance consists of a pair of spots (hot and cold) pulsating at the same azimuthal positions along the interface (Fig 12).

As discussed in Ref<sup>1</sup> these spots are responsible for thermocapillary effects in the azimuthal direction, causing a pair of counter-rotating vortex cells in the transversal section.

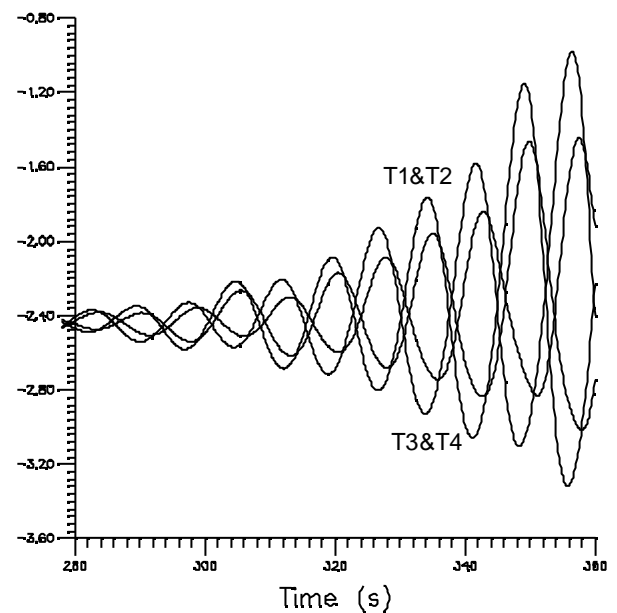


Fig 9a: Oscillations at the onset ( $\Delta T=30$  K)

At the same time strong interior temperature extrema appear, conductively heating or cooling them. As originally proposed by Smith and Davis<sup>10</sup> thermocapillary forces support this mechanism, so that the spots become pulsating (the hot spot replaces the cold one and viceversa).

When the  $\Delta T$  increases to 40 K, a travelling wave appears, characterized by two rotating temperature spots along the free surface of the liquid bridge (Figs. 13).

By looking at the liquid surface the time dependence is described by hot and cold spots rotating around the axis of the floating zone. The variation in time of the surface temperature distribution, in the oscillatory regime, shows a quite isothermal surface with hot and cold zones rotating around the bridge.

In this case the temperature disturbance is a periodic function of the time and of the azimuthal co-ordinate.

To illustrate these behaviours, four "numerical" thermocouples have been located in the bridge (Fig 9) at different azimuthal positions

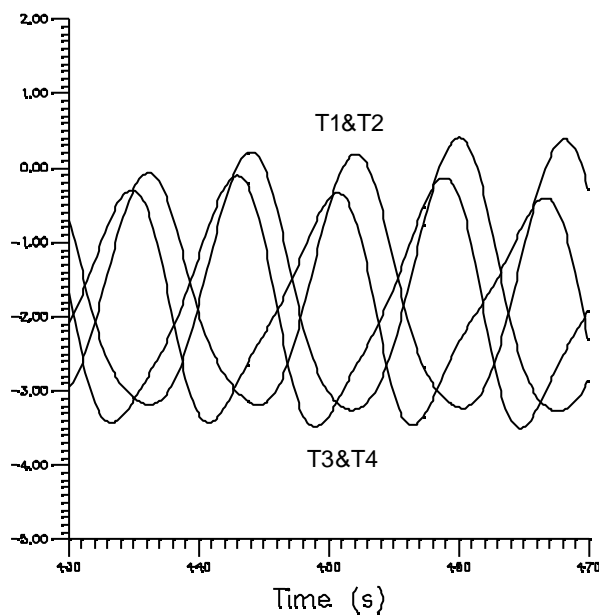


Fig 9b: Oscillations after 400 sec ( $\Delta T=30$  K)

(with a shift of 90 degree). In Fig. 9b the computed temperatures of the thermocouples T1, T2, T3 and T4, are shown for the standing wave regime ( $t = 350$  s). Fig 9c shows the results obtained for the travelling wave regime ( $t= 530$  s). For the standing wave model, it can be observed that there is no phase shift between T1 and T2 and no phase shift between T3 and T4 but T1 and T2 measure values with a phase shift of  $\pi$  respect to T3 and T4.

This behaviour can be explained considering that the temperature disturbance can be represented as two spots on the liquid bridge surface heated or cooled by stronger interior temperature extrema. In the pulsating model these spots have azimuthal fixed positions. Since for  $m=1$  the azimuthal extension of each spot is 180 degree, and the thermocouples have an azimuthal shift of 90 degree, two thermocouples will be placed on a spot and the others on the second spot measuring values having an opposite phase.

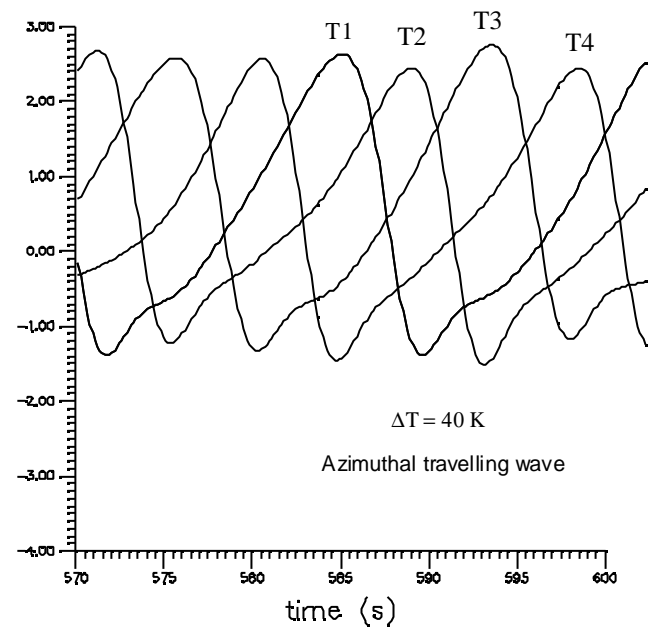


Fig 9c: Transition from standing wave model to travelling wave model when the  $\Delta T$  is increased from 30 K to 40 K

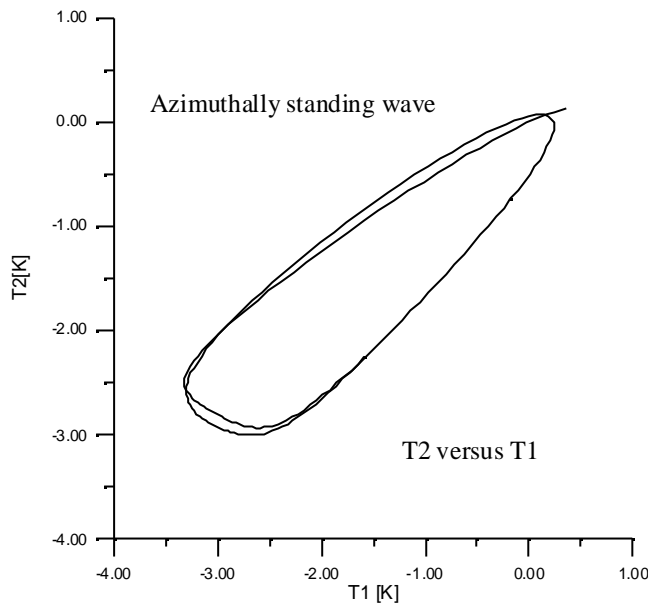


Fig 10a: T2 versus T1 after 400s ( $\Delta T=30$  K)

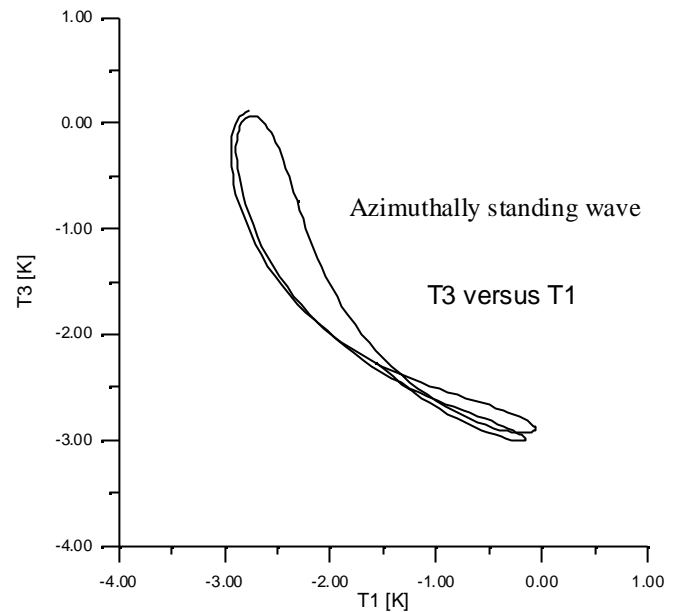


Fig 10b: T3 versus T1 after 400s ( $\Delta T=30$  K)

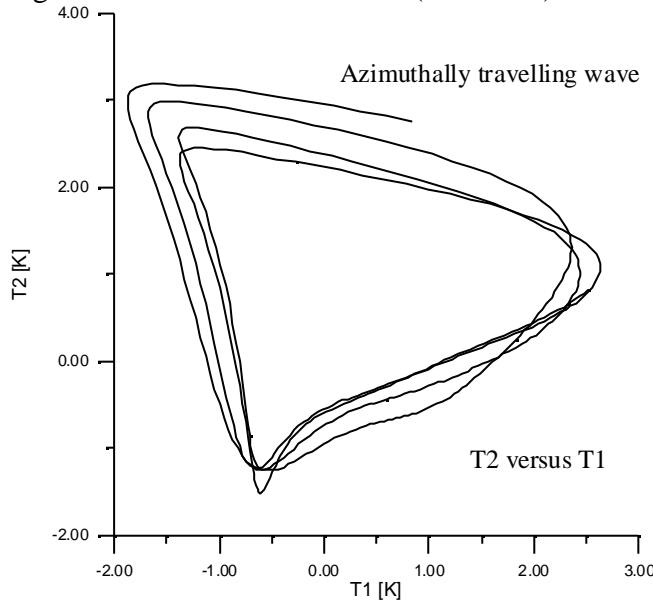


Fig 11a: T2 versus T1 after 550s ( $\Delta T=30$  K)

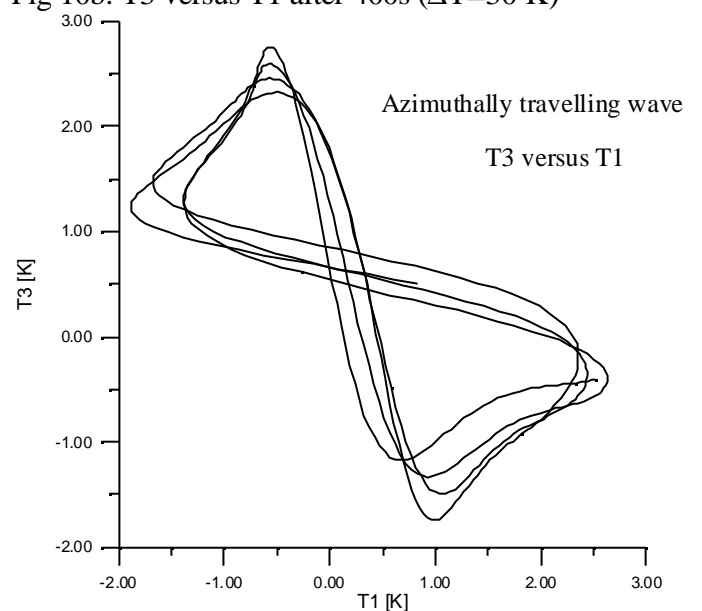


Fig 11b: T3 versus T1 after 550s ( $\Delta T=30$  K)

In the travelling wave model, the spots are not fixed, but rotate in azimuthal direction, hence each of the four numerical thermocouples measures a maximum (minimum) temperature value when the hot (cold) spot passes on it. In the rotating model the time temperature profiles show hence a phase displacement depending on the azimuthal co-ordinate. Since the critical wave number is  $m = 1$ , the oscillations show a phase displacement of  $\pi/2$  between two numerical thermocouples located at angular distance of 90 degree

and a phase displacement of  $\pi$  between two numerical thermocouples located at angular distance of 180 degree. This result agrees with the experimental observations by Presser and Schwabe<sup>6</sup> who measured the temperature oscillations by two thermocouples located at the same axial and radial co-ordinates, but at different azimuthal co-ordinates, and found that the temperatures oscillate synchronously with the same frequency and a phase shift  $\Delta\theta$  depending on the azimuthal distance  $\Delta\phi$ .

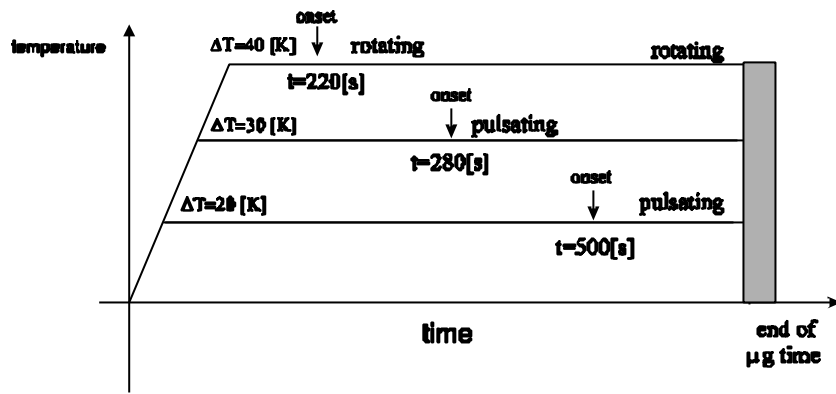


Fig 14: relation between the  $\Delta T$  and the nature of bifurcation of Marangoni flow

The critical wave number was experimentally determined as  $m = \Delta\phi / \Delta\varphi = 1$  (ratio of the phase shift and of the azimuthal shift)

It should be noted that the numerical simulation have shown that increasing  $\Delta T$  from 30 K to 40 K accelerates the transition from pulsating model to rotating one is but the critical wave number does not change ( $m=1$ ). A stronger increase in  $\Delta T$  ( $> 40$  K) is to avoid because according to linear stability theory it could give rise to a bifurcation to a  $m=2$  (or higher) mode.

The numerical computation show that for  $\Delta T = 30$  K when a standing wave oscillatory pulsating mechanism is completely developed the temperature difference can be further increased so that the transition to the rotating instability is accelerated.

Fig 14 show the expected times at which transition occurs at fixed different  $\Delta T$ .

If the experiment is pre-programmed, it is possible to get only one transition to oscillatory condition.

The short duration mission requires an optimization of the experiment sequence, that can be achieved only by controlling the experiment from the ground through a direct interaction with the PI.

The basic idea of the experiment is to change the parameters and conditions to get both the transitions.

The first transition can be obtained at  $\Delta T = 30$  [K]; after the pulsating mode is clearly established and recorded, the PI should increase the  $\Delta T$  to 40 [K] to get at the end of the  $\mu g$  time the transition to rotating flow.

Transition from one regime to another will be detected by the PI from the visual observation of the flow field through the light cut illumination of the liquid bridge and by looking at the thermocouples output versus time and by cross correlating the temperatures at different azimuthal points (Fig.10 , Fig. 11 and Fig. 15).

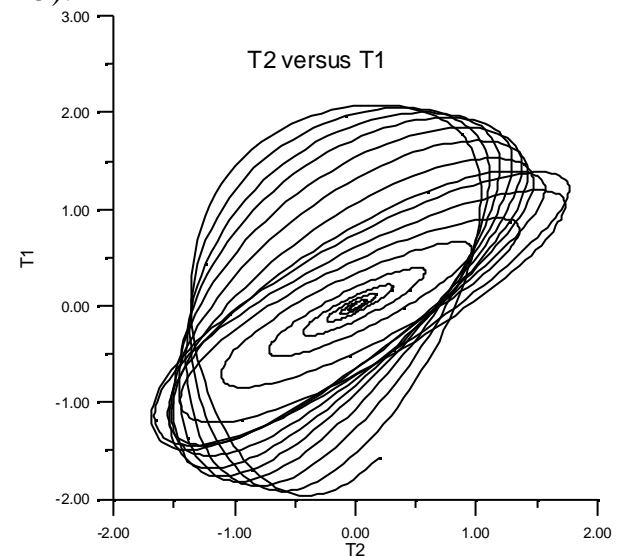


Fig 15: T2 versus T1 from the onset of the oscillations to the end of the available microgravity time

## 4. Conclusions

The numerical computations show that for the configuration to be investigated during the microgravity experiment, if the imposed temperature difference is sufficiently small (but larger than the critical one), the three-dimensional instability starts as a standing wave ( $m=1$ ) and the pulsating mechanism last for a time larger than the available microgravity time.

Conversely, if the the imposed temperature difference is sufficiently large the bifurcation gives rise to a travelling wave ( $m=1$ ) and no transition can be observed from the pulsating to the rotating instability mechanism .

Since the the objective of the experiment is to get both the pulsating and the rotating instabilities, a different experimental procedure has been investigated numerically: a pulsating instability is first achieved by imposing a suitable temperature difference with a relatively fast temperature ramp; when this oscillatory mechanism is completely developed the temperature difference is further increased so that the transition to the rotating instability is established.

The numerical computations show that this procedure, that requires real-time remote control of the experiment is the best one for the optimum utilization of the available microgravity time.

The experimental results in the case of the microscale confirm the main result of the numerical simulations performed in the case of the bridge  $L=20$  mm  $D=20$  mm i.e. that for a suitable  $\Delta T$  the instability starts as a standig wave and then develops in a travelling wave and that the transition can be anticipated increasing the  $\Delta T$ .

Moreover, the influence of buoyancy forces on the stability and on the bifurcation process has been investigated

by heating the bridge from above and from below. The direct comparison of these two heating conditions indicates that the critical  $\Delta T$  obtained when heating from below are always larger than those found when heating from above. This behaviour is intriguing by is confirmed but the numerical analyses performed in this paper.

## 5. References

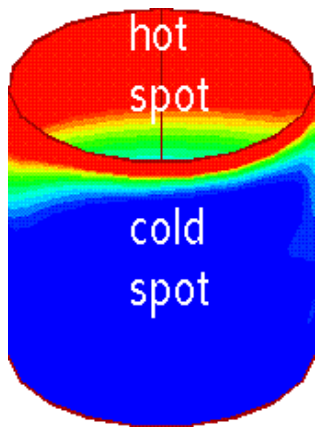
- <sup>1</sup>R. Savino and R. Monti, Oscillatory Marangoni convection in cylindrical liquid bridges, *Phys. Fluids*, 1996
- <sup>2</sup>R. Savino and R. Monti, Three-dimensional numerical simulation of thermocapillary instabilities in floating zones, *Applied Scientific Reserch*, 1996, 56: 19-41
- <sup>3</sup>R.Monti,R.Savino and M.Lappa: "Oscillatory Thermocapillary flows in simulated floating zones with time-dependent boundary conditions" ; 47th International Astronautical Federation congress, in press on *Acta Astronautica*.
- <sup>4</sup>Kuhlmann H.C., Rath H.J. 1993, Hydrodynamic instabilities in cylindrical thermocapillary liquid bridges, *J. Fluid Mechanics*, vol. 247, 247-274
- <sup>5</sup>M.Wanschura, V. Shevtsova, H.C.Kuhlmann H.C., Rath H.J. 1995, Convective instability mechanism in thermocapillary liquid bridges, *Phys. Fluids A* vol. 5, 912-925
- <sup>6</sup>Preisser F., Schwabe D., Scharmann A., 1983, Steady and oscillatory Marangoni convection in liquid colums with free cylindrical surface, *J. Fluid Mechanics*, 126, 545
- <sup>7</sup>C.H.Chun , W.West, 1979, Experiments on the transition from the steady to the oscillatory Marangoni convection of a floating zone under reduced gravity effect, *Acta Astronautica* Vol 6 , pp 1073-1082
- <sup>8</sup>Velten R., Schwabe D., Scharmann A. 1991, The periodic instability of thermocapillary convection in cylindrical liquid bridges, *Phys. Fluids A* 3, 267-279
- <sup>9</sup>Monti R. et al., 1995, First Results from "Onset" Experiment during Spacelab Mission D-

2, Scientific Results of the German Spacelab Mission D-2

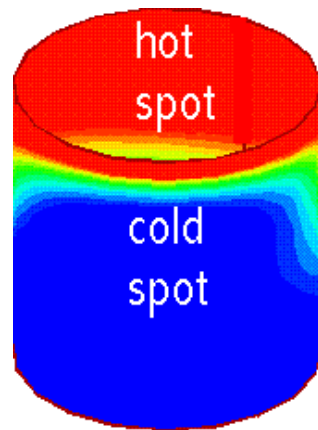
<sup>10</sup>Smith M.K., Davis S.H., 1983, Instability of dynamic thermocapillary liquid layers. *J. Fluid Mechanics*, 132, 119

<sup>11</sup>J.J.Xu and S.H.Davis, 1984, Convective thermocapillary instabilities in liquid bridges, *Phys. Fluids* 27, 1102

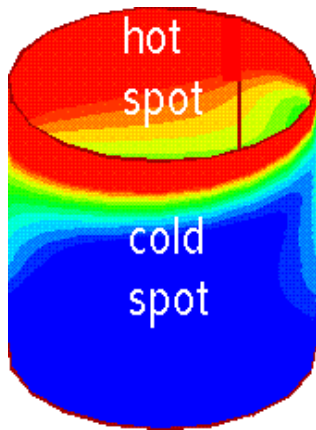
<sup>12</sup>Monti R., Savino R., 1994, Effect of unsteady thermal boundary conditions on Marangoni flow in liquid bridges. *Microgravity Quarterly*, 4, 163



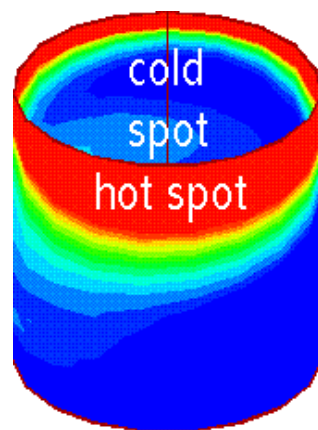
12a)



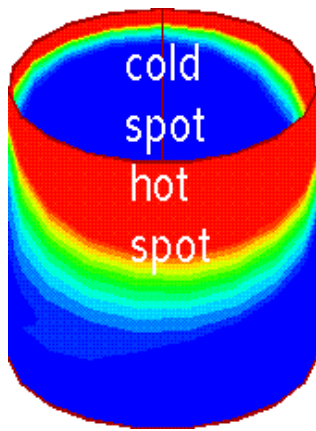
12b)



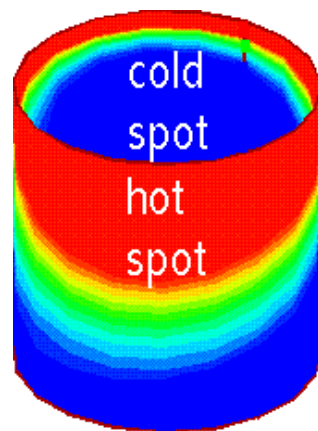
12c)



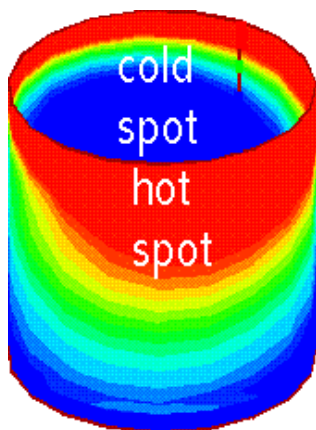
12d)



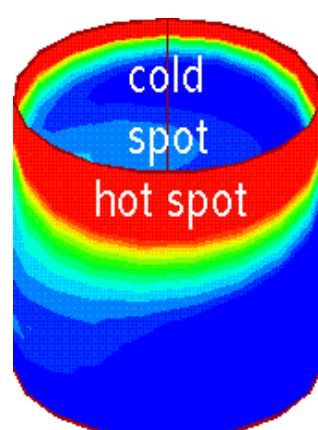
12e)



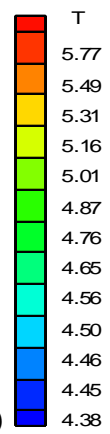
12f)

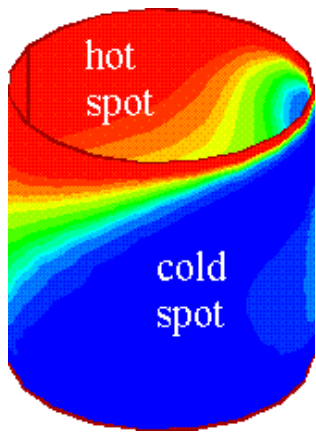


12g)

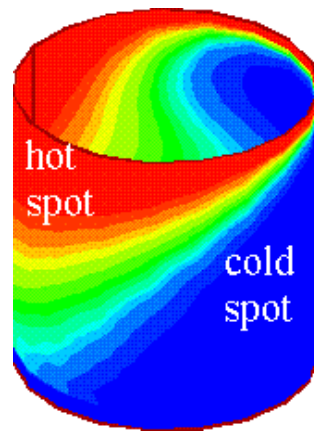


12h)

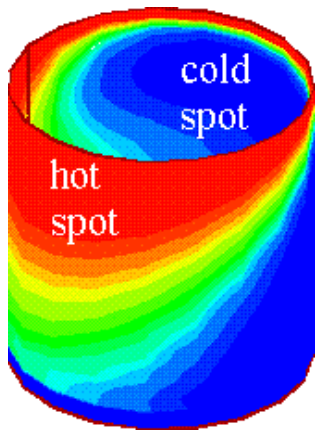




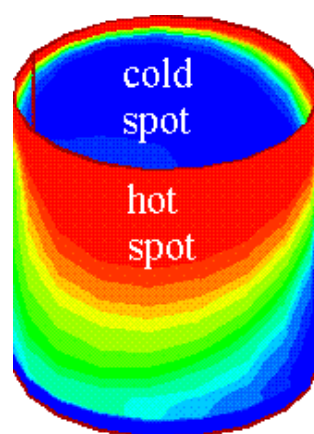
13a)



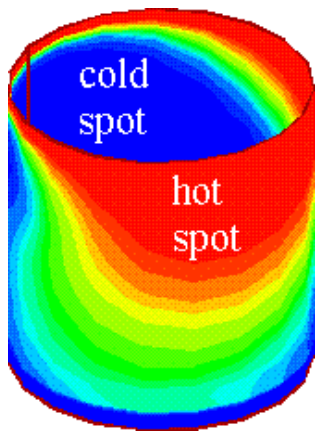
13b)



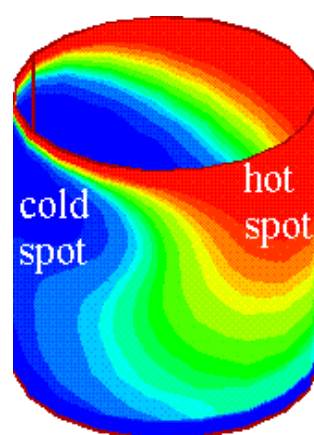
13c)



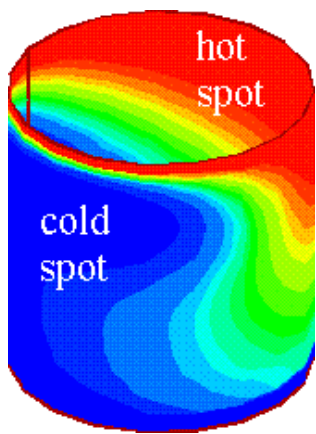
13d)



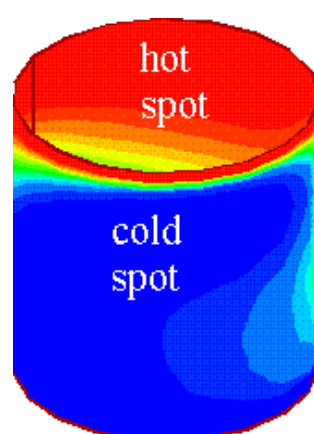
13e)



13f)



13g)



13h)

